Supplementary 1 (Related to Figure 1)

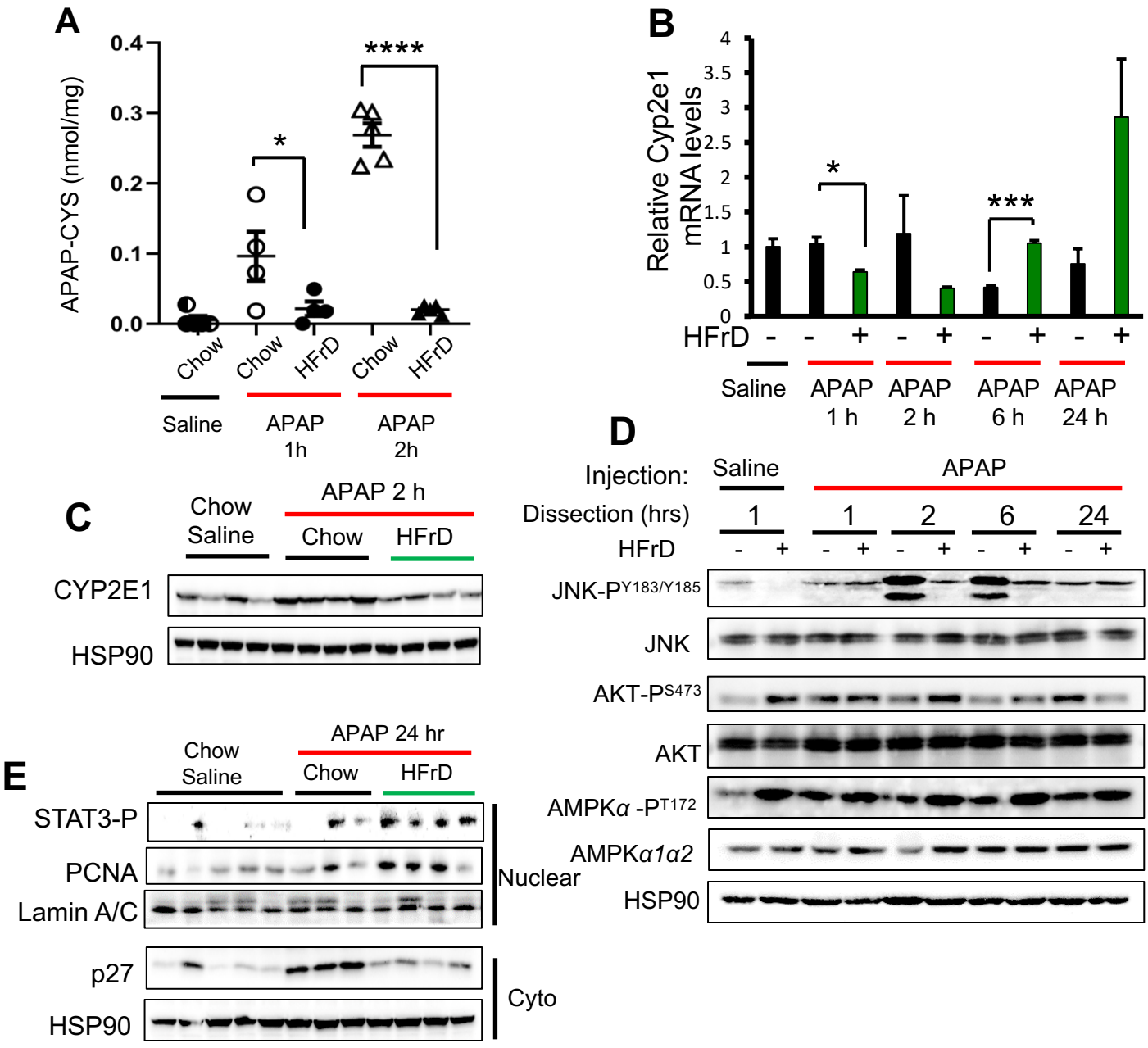

Supplementary 1 (Related to Figure 1)**. Impact of HFrD feeding on the APAP-protein adduct formation, CYP2E1 expression, survival kinases, and liver regeneration markers in the liver after APAP injection**. Mice were treated as described in **Figure 1** (n = 4-5). (**A**) APAP-protein adduct levels in the liver were assessed for mice dissected 1 hr and 2 hrs after APAP injection. (**B**) Hepatic *Cyp2e1* mRNA levels were assessed by RT-qPCR for all time points. (**C**) Hepatic CYP2E1 protein levels were assessed by western blot for mice dissected 1 hr after APAP injection. (**D**) phosphorylation levels of JNK, AKT and AMPK in the liver were assessed by western blotting for all time points. (**E**) Liver re-generation markers including STAT3 phosphorylation, PCNA, and p27 were assessed by western blotting for mice dissected 24 hrs after APAP injection. *$p < 0.05$; *** $p < 0.001$; **** $p < 0.0001$ by one-way ANOVA with Tukey's test. These data are presented as Mean ± SEM.

Supplementary 2. (Related to Figure 1)

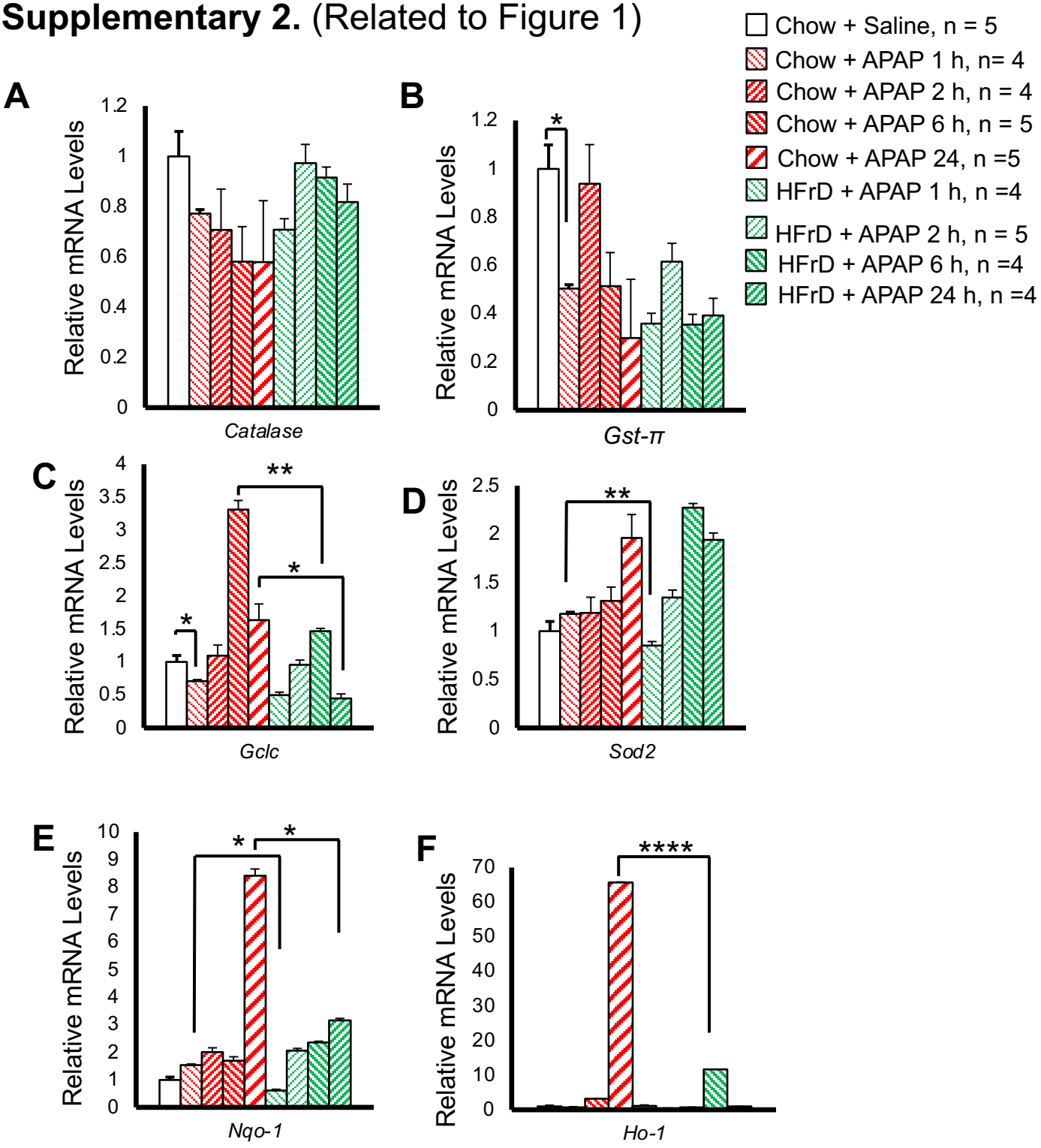

Supplementary 2 (Related to Figure 1)**. Impact of HFrD feeding on the NRF-2 pathway genes in the liver after APAP injection**. Mice were treated as described in **Figure 1**. NRF2 pathway in the liver were assessed by RT-qPCR.*$p < 0.05$; ** $p < 0.01$; **** $p < 0.0001$ by one-way ANOVA with Tukey's test. These data are presented as Mean ± SEM.

Supplementary 3. (Related to Figure 2)

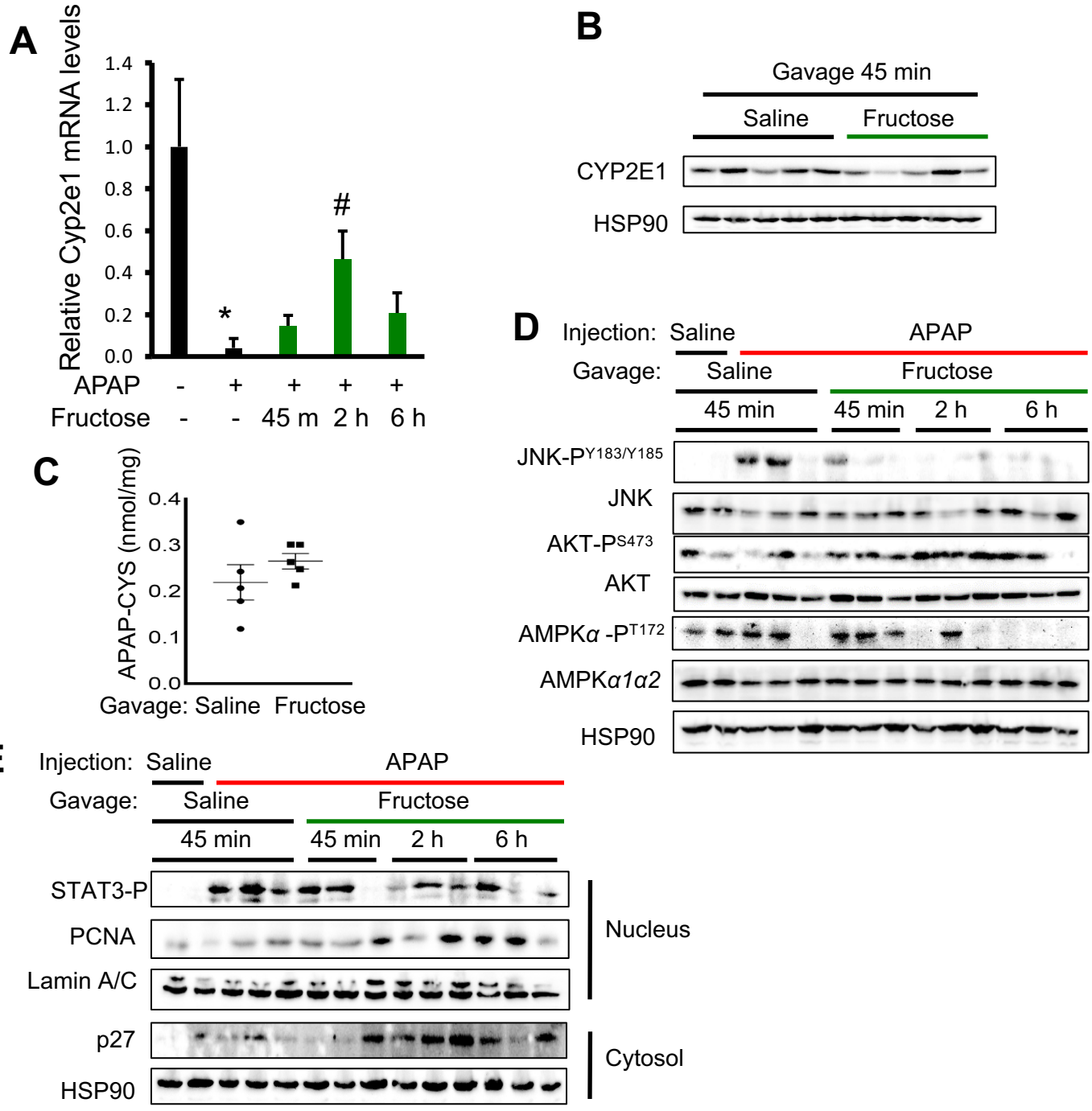

Supplementary 3 (Related to Figure 2)**. Impact of HFrD feeding on the NRF-2 pathway genes in the liver after APAP injection**. Mice were treated as described in **Figure 2** (n = 4-5). (**A**) Cyp2e1 mRNA levels were assessed by RT-qPCR. (**B-C**) 8-week male mice were injected with APAP, gavaged with fructose 45 minutes later, and sacrificed 2 hrs later to collect liver for CYP2E1 protein (**B**) and APAP-protein adduct level assessment (**C**). (**D**) phosphorylation levels of JNK, AKT and AMPK in the liver were assessed by western blotting for representative mice of each time point. (**E**) Liver re-generation markers including STAT3 phosphorylation, PCNA, and p27 were assessed by western blotting for representative mice of each time point. *p < 0.05 for APAP+Saline vs. Saline+Saline; # p < 0.05 for APAP+Fructose vs. APAP+Saline by one-way ANOVA with Tukey's test. These data are presented as Mean ± SEM.

Supplementary 4. (Related to Figure 2)

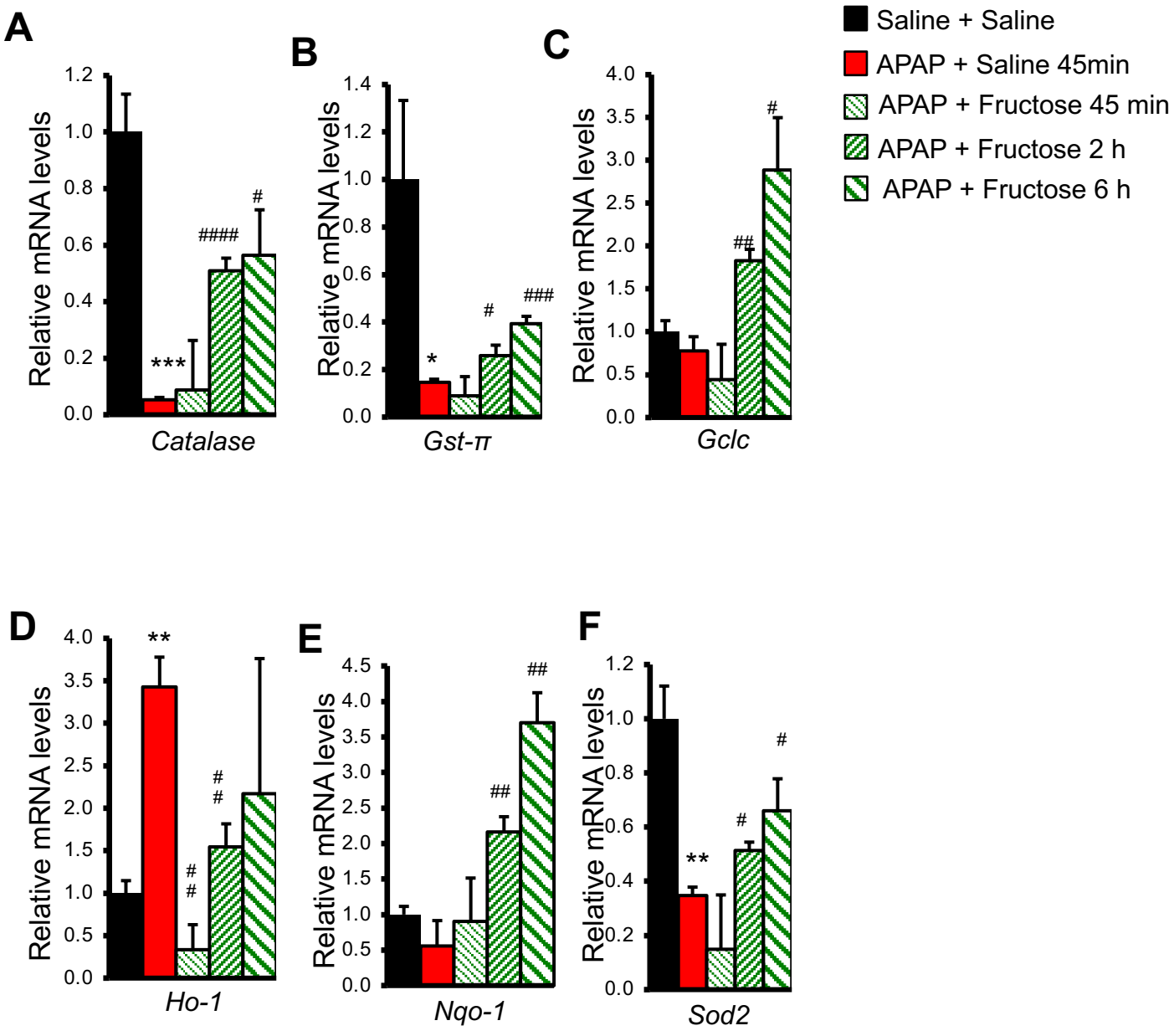

Supplementary 4 (Related to Figure 2)**. Impact of fructose gavage on the NRF2 pathway genes in the liver after APAP injection**. Mice were treated as described in **Figure 2**. Hepatic genes in the NRF2 pathway were assessed by RT-qPCR.* Saline+Saline *v.s.* APAP+Saline, # APAP+Fructose *v.s.* APAP+Saline. *$p < 0.05$; ** $p < 0.01$; *** $p < 0.001$ by one-way ANOVA with Tukey's test. These data are presented as Mean ± SEM.

Supplementary 5.

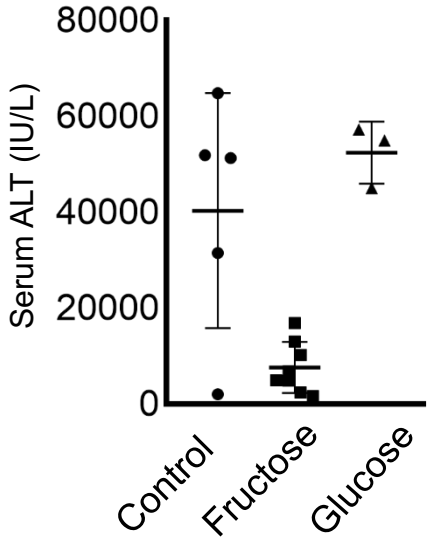

Supplementary 5. Glucose gavage shows no protection against APAP-induced liver injury. 8-week male mice were gavaged with water, fructose (4.5 g/kg), or glucose (4 g/kg) 45 minutes after intraperitoneal injection with APAP, and sacrificed 6 h later for tissue collecting (n= 4 for water, n= 8 for fructose, and n = 3 for glucose). Serum ALT level was measured to assess liver injury.

Supplementary 6.

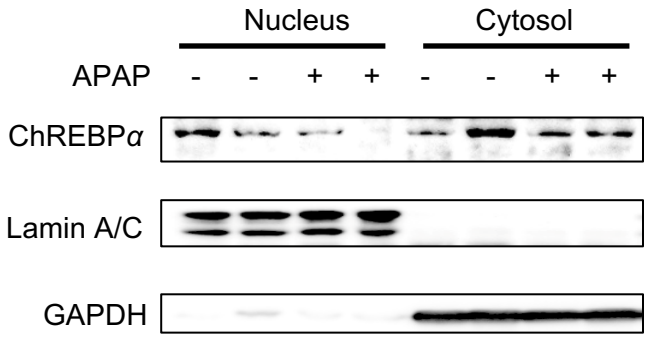

Supplementary 6 (Related to Figure 3)**. Abundance of ChREBPα in both nuclear and cytosolic fractions in the mouse liver with saline or APAP injection**. The same amounts of nuclear fraction and cytosol fraction from the livers of saline or APAP injected mice were loaded for immuno-blotting to detect ChREBPα, Lamin A/C, and GAPDH (n=2 per group).

Supplementary 7. (Related to Figure 5)

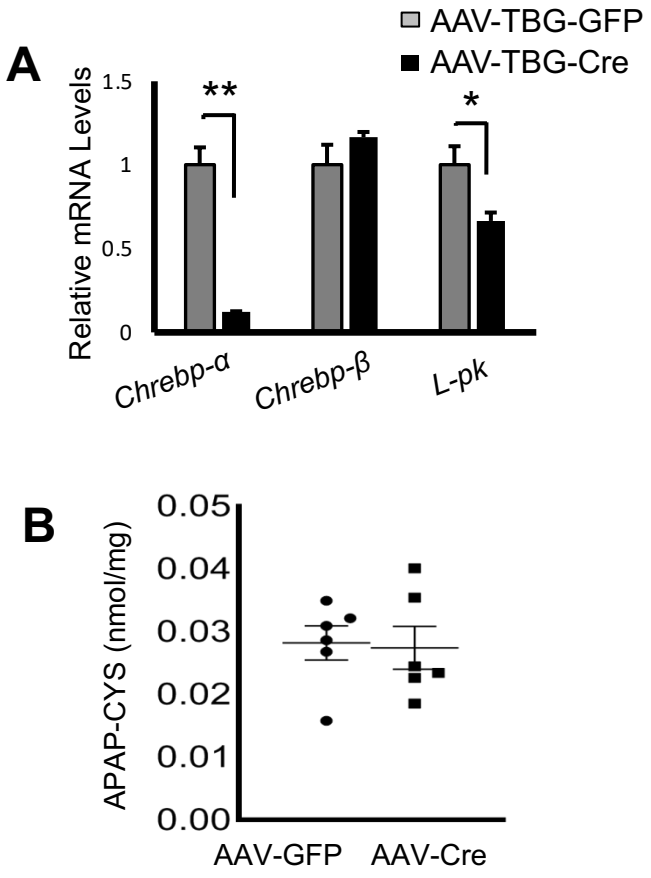

Supplementary 7 (Related to Figure 5)**. Impact of liver-specific deletion of *Chrebpα* on the levels of ChREBP target expression and the APAP-protein adducts in the mouse liver after APAP injection**. (**A**) Primary hepatocytes were isolated from *Chrebp*$^{flox/flox}$ mice injected with AAV-TBG-GFP or AAV-TBG-Cre, and subjected to RT-qPCR for mRNA levels of ChREBPα and its targets *Chrebp-β* and *L-pk*. ((**B**) *Chrebp*$^{flox/flox}$ mice were injected with AAV-TBG-GFP or AAV-TBG-Cre, and feed HFrD for 2 weeks. Then the mice were injected with APAP, and 2 hrs later the livers were collected for APAP-protein adducts assessment. *$p < 0.05$; ** $p < 0.01$ by two-tailed Student's *t*-test. These data were presented as Mean ± SEM.

Supplementary 8 (Related to Figure 6)

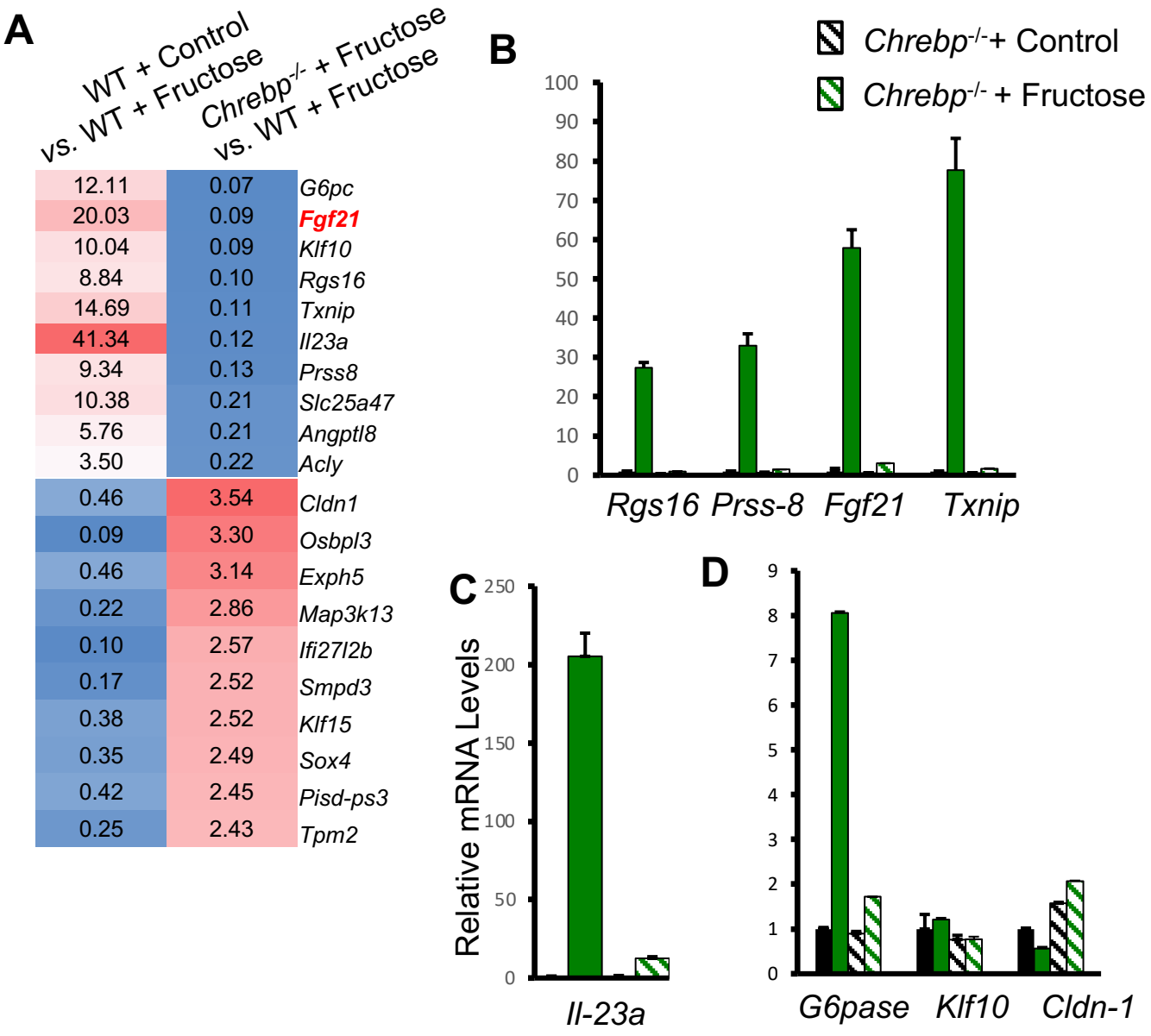

Supplementary 8 (Related to Figure 6)**. identification of *Fgf21* as one of the top fructose-activated genes via ChREBP**α. Primary mouse hepatocytes were isolated from the liver of wildtype and *Chrebp*$^{-/-}$ mice, and cultured in medium supplemented with or without 25 mM fructose for 16 hrs. Each treatment was performed in duplicate. The cells were then subjected to RNA extraction and Affymetrix Microarray. (**A**) Genes up-regulated or down-regulated by fructose in wildtype but not *Chrebp*$^{-/-}$ primary mouse hepatocytes are listed. (**B-D**) Expression level changes identified by microarray were verified by RT-qPCR. These data are presented as Mean ± SEM.

Supplementary 9 (Related to Figure 6)

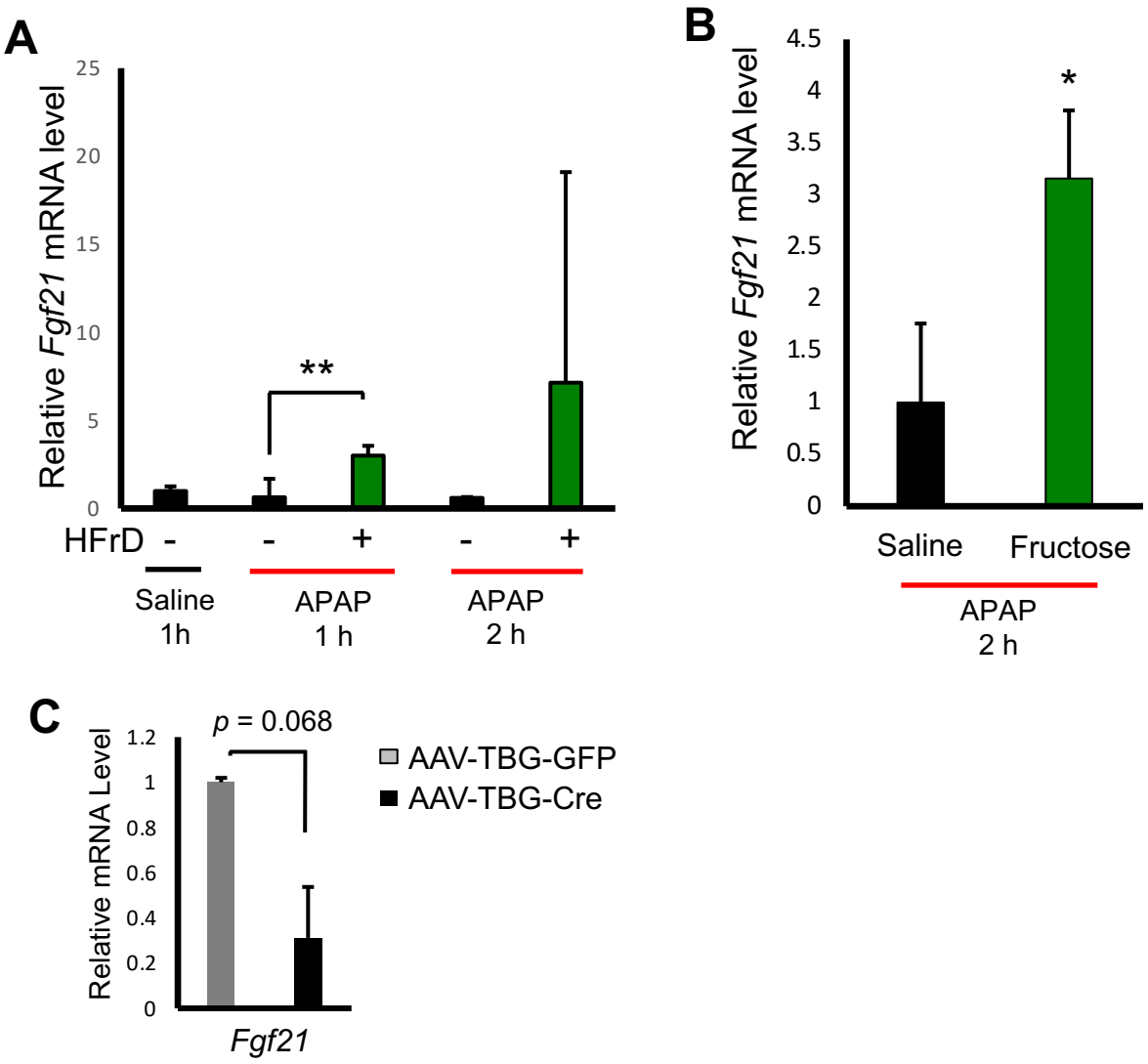

Supplementary 9 (Related to Figure 6). **Hepatic *Fgf21* mRNA is induced by both HFrD feeding before APAP injection and fructose gavage after APAP injection.** (**A**) Mice were treated as described in Figure 1. *Fgf21* mRNA level in the liver was determined by RT-qPCR for mice dissected 1 hr and 2 hrs post APAP or saline injection. (**B**) 8-week male mice were injected with APAP, gavaged with fructose 45 min later, and sacrificed 2 hrs later for tissue collecting. Liver *Fgf21* mRNA level was determined by RT-qPCR. (**C**) *Chrebp*$\alpha^{flox/flox}$ mice were treated as described in Figure 5, and *Fgf21* mRNA level were assessed in the liver. ** $p < 0.01$ by one-way ANOVA with Tukey's test for (**A**). * $p < 0.05$ by two-tailed Student's *t*-test for (**B**). These data are presented as Mean ± SEM.

Supplementary 10. (Related to **Figure 6D**)

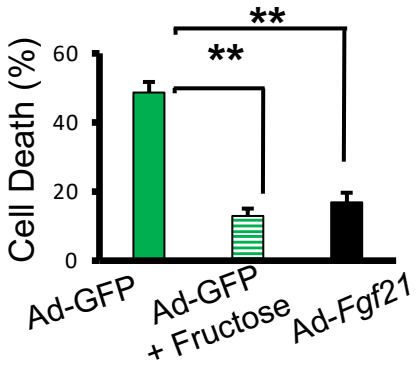

Supplementary 10 (Related to Figure 6D)**. Both Fructose and FGF21 overexpression suppress APAP-induced cell death in hepatocytes.** Primary mouse hepatocytes were treated as described as in **Figure 6D**. The percentage of apoptotic cells was determined by normalizing TUNEL positive cells to DAPI counts. n = 3, ** $p < 0.01$ by one-way ANOVA followed with Tukey's test. These data are presented as Mean ± SEM.

Supplementary 11. (Related to **Figure 6F**)

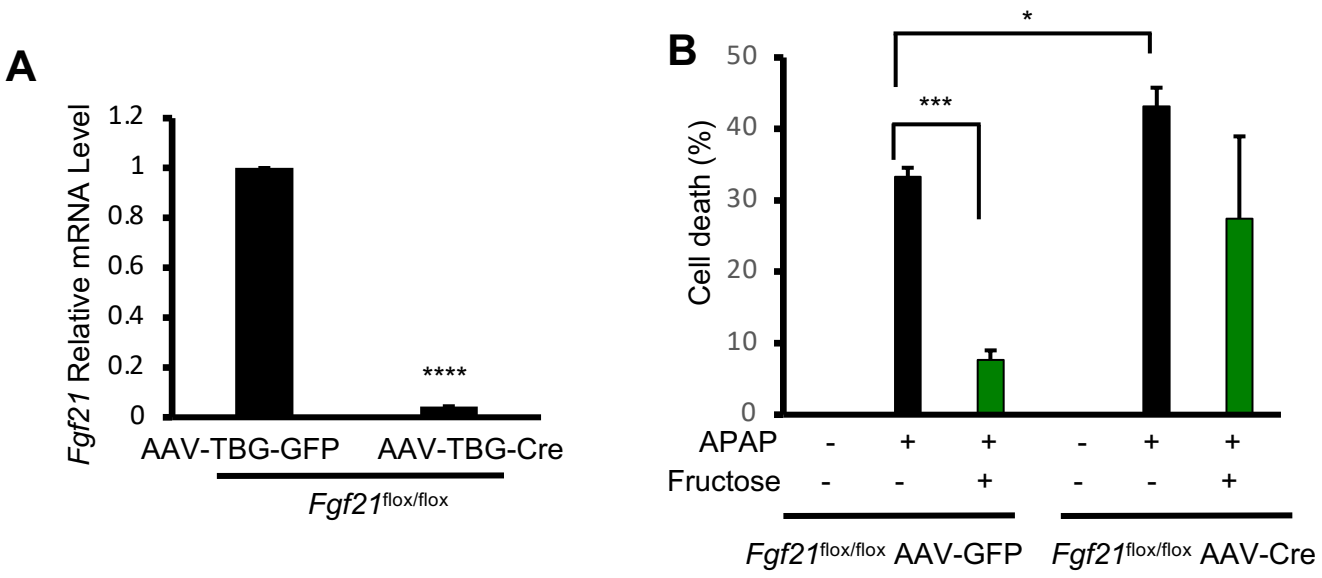

Figure 11 (Related to Figure 6F). (**A**) **Verification of Cre-mediatedFgf21 deletion by RT-qPCR in hepatocytes**. Primary mouse hepatocytes were treated as described as in Figure 6F. The *Fgf21* deletion efficiency were determined by RT-qPCR for *Fgf21*. (**B**) **Quantification of APAP-induced cell death in hepatocytes in Figure 6F.** Figure The percentage of dead cells was determined by normalizing TUNEL positive cells to DAPI counts (**B**). **** $p < 0.0001$ by two-tailed Student's *t*-test for (**A**), * $p < 0.05$, *** $p < 0.001$ by one-way ANOVA with Tukey's test for (**B**). These data are presented as Mean $\pm$ SEM.

Supplementary 12. (Related to **Figure 7**)

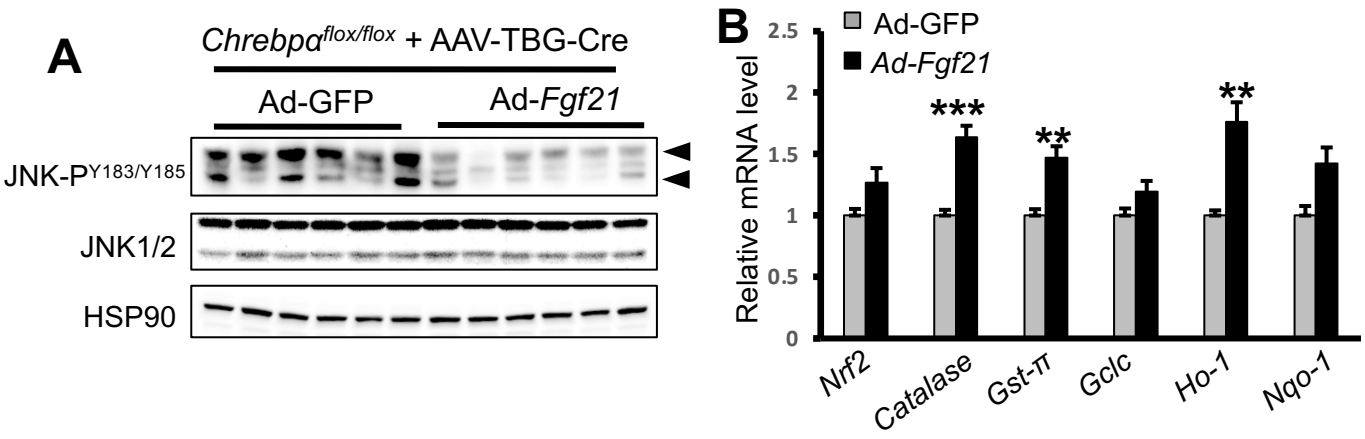

Supplementary 12 (Related to Figure 7)**.** Effects of overexpression of hepatic Fgf21 on the JNK kinase activation and the NRF2 pathway gene expression in the APAP-injected mouse liver. (**A**) The JNK phosphorylation and total levels were assessed by western blotting. (**B**) NRF2 pathway in the liver were assessed by RT-qPCR. ** $p < 0.01$; *** $p < 0.001$ by two-tailed Student's *t*-test. These data were presented as Mean ± SEM.